Journal of Physics D:
Applied Physics

PAPER • **OPEN ACCESS**

Vibrational CARS measurements in a near-atmospheric pressure plasma jet in nitrogen: II. Analysis

To cite this article: J Kuhfeld *et al* 2021 *J. Phys. D: Appl. Phys.* **54** 305205

OPEN ACCESS
IOP Publishing
Journal of Physics D: Applied Physics
J. Phys. D: Appl. Phys. **54** (2021) 305205 (10pp)
https://doi.org/10.1088/1361-6463/abfd6c

Vibrational CARS measurements in a near-atmospheric pressure plasma jet in nitrogen: II. Analysis

J Kuhfeld*, D Luggenhölscher and U Czarnetzki*

Ruhr University Bochum, Institute for Plasma and Atomic Physics, Bochum, Germany

E-mail: jan.kuhfeld@rub.de and uwe.czarnetzki@rub.de

Received 26 January 2021, revised 7 April 2021
Accepted for publication 30 April 2021
Published 25 May 2021

Abstract

The understanding of the ro-vibrational dynamics in molecular (near)-atmospheric pressure plasmas is essential to investigate the influence of vibrational excited molecules on the discharge properties. In a companion paper Kuhfeld *et al* (2021 *J. Phys. D: Appl. Phys.* **54** 305204), results of ro-vibrational coherent anti-Stokes Raman scattering (CARS) measurements for a nanosecond pulsed plasma jet consisting of two conducting molybdenum electrodes with a gap of 1 mm in nitrogen at 200 mbar are presented. Here, those results are discussed and compared to theoretical predictions based on rate coefficients for the relevant processes found in the literature. It is found, that during the discharge the measured vibrational excitation agrees well with predictions obtained from the rates for resonant electron collisions calculated by Laporta *et al* (2014 *Plasma Sources Sci. Technol.* **23** 065002). The predictions are based on the electric field during the discharge, measured by electric field induced second harmonic generation Kuhfeld *et al* (2021 *J. Phys. D: Appl. Phys.* **54** 305204), Lepikhin *et al* (2020 *J. Phys. D: Appl. Phys.* **54** 055201) and the electron density, which is deduced from the field and mobility data calculated with Bolsig+ Hagelaar and Pitchford (2005 *Plasma Sources Sci. Technol.* **14** 722–33). In the afterglow a simple kinetic simulation for the vibrational subsystem of nitrogen is performed and it is found, that the populations of vibrational excited states develop according to vibrational-vibrational transfer on timescales of a few microseconds, while the development on timescales of some hundred microseconds is determined by the losses at the walls. No significant influence of electronically excited states on the populations of the vibrational states visible in the CARS measurements ($v \lesssim 7$) was observed.

Keywords: nitrogen plasma, ro-vibrational excitation, CARS, nanosecond discharge, APPJ, vibrational distribution function

(Some figures may appear in colour only in the online journal)

* Authors to whom any correspondence should be addressed.

1. Introduction

In recent years, (near-)atmospheric pressure plasmas have gained a lot of interest in the plasma community due to their numerous possible applications. Those plasmas often employ relatively complex gas mixtures including molecular gases. Depending on the discharge conditions a significant amount of the energy input can be stored in the vibrational excitation of molecules, which can potentially enhance chemical reactions leading to possible use cases in plasma chemistry [1] and plasma catalysis [2, 3]. To investigate the influence of the vibrational excitation it is critical to know the vibrational distribution function. Besides tunable diode laser absorption spectroscopy, Fourier transform infrared spectroscopy and spontaneous Raman scattering, coherent anti-Stokes Raman scattering (CARS) is a popular technique to measure the vibrational excitation in gaseous media which was already employed in plasmas in the past [4]. Nonetheless, CARS has a drawback in the sense that the measured signal does depend on the population differences between vibrational states, i.e. the populations cannot be determined directly from the measured CARS spectra. This is not a major problem for equilibrium systems where the vibrational population densities follow a Boltzmann distribution: with the knowledge of the distribution function theoretical CARS spectra can be calculated and fitted to measured ones with the temperature as fitting parameter [5]. The use of a simple Boltzmann distribution function is not possible in non-equilibrium systems as low-temperature plasmas, how ever. Here, several different evaluation methods were used in the past. One approach is to estimate the population density of one state and use this as starting point to calculate the others with the population differences obtained from the CARS spectra. This is done for example in an early work related to CARS in plasmas by Shaub *et al* [6] where the densities of the first two vibrational states were estimated by assuming a Boltzmann distribution for those. In other works [7, 8] it is assumed that the upper state for the highest detectable transition is approximately zero. The latter approximation is certainly reasonable for vibrational temperatures close to room temperature where the ratio between two neighboring states is about $\frac{N_{v+1}}{N_v} \approx \exp\left(-\frac{\hbar\omega_e}{k_B T_{vib}}\right) \approx 1.2 \times 10^{-5}$ with $\omega_e \approx 2359\ \mathrm{cm}^{-1}$ and $T_{vib} = 300$ K. This changes drastically for higher temperatures, e.g. $T_{vib} = 5000$ K where $\frac{N_{v+1}}{N_v} \approx 0.5$. For this reason in our companion paper [9] a different approach is used. Similar to CARS measurements in thermal equilibrium a distribution function is assumed for fitting theoretical spectra to measured ones, like it was done already by Messina *et al* [10] in a plasma burner. They assume that both the vibrational and the rotational degree of freedom are Boltzmann distributed, but have different temperatures. This works reasonably well for their measurements as they measure only up to the third vibrational state. In our measurements in [9] and previous CARS measurements in different plasma sources it can be seen, that usually the higher vibrational states are overpopulated compared to a Boltzmann distribution determined by the first two or three vibrational states. For this reason a distribution function is chosen which includes two vibrational temperatures and one rotational, either called vibrational two-temperature distribution or simply two-temperature distribution function (TTDF) in the following. As the TTDF is motivated by the underlying plasma physics in the discharge, a detailed derivation was omitted in [9] where the focus was on the diagnostic method. In the present paper we motivate the use of the TTDF based on the excitation processes in the plasma in section 3.1. Additionally, simple models are derived for the parameters in the TTDF connecting them to the plasma parameters. Finally, the population difference results from [9] in the afterglow where the TTDF is not valid anymore are compared to a simple kinetic model for the vibrational subsystem in section 3.2.

2. Summary of the results in [9]

In [9] a ns-pulsed discharge with a parallel electrode configuration is studied. The discharge jet consists of two molybdenum electrodes with a length of 20 mm and a thickness of 1 mm. The 1 mm gap between the electrodes is enclosed with two glass plates at the long edges of the electrodes. In the middle of one glass plate a hole with about 1 mm diameter serves as gas inlet. This way two opposing gas channels with a 1 mm$\times$ 1 mm cross section and 10 mm length are constructed. By applying a high voltage to one of the electrodes, while grounding the other, an electric field can be created transverse to the gas flow. This geometry was chosen to provide a simple model geometry for nanosecond pulsed discharges in a pressure range close to atmospheric pressure (about 100 mbar up to 1 bar). It should be noted that in contrast to the dielectric barrier discharges (DBD) more often used to operate nanosecond pulsed plasmas around atmospheric pressure, here a conduction current can flow for as long as several hundred nanoseconds depending on the power supply. This was seen to have major impact on the vibrational excitation in [9].

The discharge is operated in pure nitrogen at a pressure of 200 mbar and a gas flow of 20 sccm. A high voltage pulse is applied with 200 ns or 250 ns pulse length (see figure 1) and a repetition rate of 1 kHz. The applied voltages lead to the current waveforms depicted in figure 1 with a high current peak during the ignition of the discharge and a relatively constant, lower current plateau for the remainder of the discharge pulse due to a voltage drop across a series resistor. These conditions produce a homogeneous discharge along the gas channel without arcing. The electric field is measured in the middle of the discharge gap at multiple times during the constant current plateau via the electric field induced second harmonic generation (E-FISH) technique and measurements of the rovibrational distributions are performed by CARS during the discharge pulse and in the afterglow between two pulses for three different voltage pulses shown in figure 1. The electric field is found to be around 81 Td at all times during the current plateau for all three discharge conditions. For the analysis of the measured CARS spectra a vibrational two-temperature distribution of the form

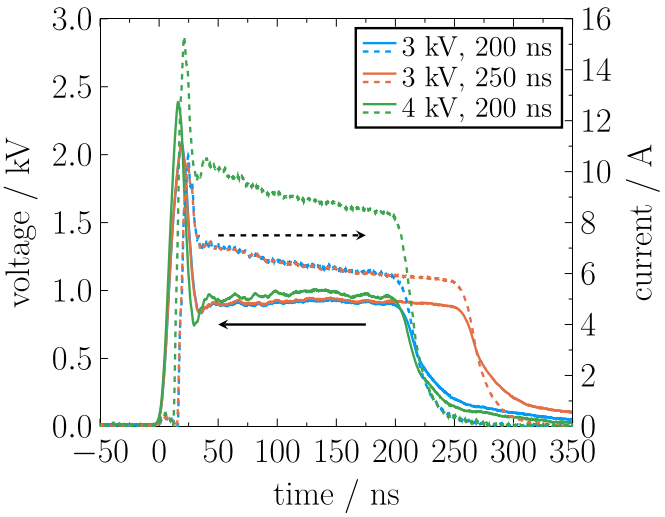

Figure 1. Voltages (solid) and currents (dashed) at the cathode used for the measurements in [9].

$$N(v,J;T_{\mathrm{rot}},T_{\mathrm{vib,c}},T_{\mathrm{vib,h}},R_{\mathrm{h}}) = g(J)\mathrm{e}^{-\frac{E(v,J)-E(v,0)}{k_{\mathrm{B}}T_{\mathrm{rot}}}}\left[\frac{1-R_{\mathrm{h}}}{Z_{\mathrm{c}}}\mathrm{e}^{-\frac{E(v,0)-E(0,0)}{k_{\mathrm{B}}T_{\mathrm{vib,c}}}} + \underbrace{\frac{R_h}{Z_h}\mathrm{e}^{-\frac{E(v,0)-E(0,0)}{k_{\mathrm{B}}T_{\mathrm{vib,h}}}}}_{\text{for } v>0}\right] \quad (1)$$

is proposed, which distinguishes between the rotational(-translational) temperature T_{rot} and two vibrational temperatures—$T_{\mathrm{vib,c}}$ for a vibrationally cold distribution and $T_{\mathrm{vib,h}}$ for a smaller, vibrationally hot distribution. For nitrogen the degeneracy of the rotational states is

$$g(J) = \begin{cases} 6(2J+1), & \text{if } J \text{ even} \\ 3(2J+1), & \text{if } J \text{ odd.} \end{cases} \quad (2)$$

The partition function for the vib. cold molecules is given by

$$Z_{\mathrm{c}} = \sum_{v,J} g(J)\mathrm{e}^{-\frac{E(v,J)-E(v,0)}{k_{\mathrm{B}}T_{\mathrm{rot}}}} \times \mathrm{e}^{-\frac{E(v,0)-E(0,0)}{k_{\mathrm{B}}T_{\mathrm{vib,c}}}} \quad (3)$$

and for the vib. hot molecules by

$$Z_{\mathrm{h}} = \sum_{v>0,J} g(J)\mathrm{e}^{-\frac{E(v,J)-E(v,0)}{k_{\mathrm{B}}T_{\mathrm{rot}}}} \times \mathrm{e}^{-\frac{E(v,0)-E(0,0)}{k_{\mathrm{B}}T_{\mathrm{vib,h}}}}. \quad (4)$$

A detailed motivation of this distribution function is given in section 3.1 where also the measurement results are presented in figures 7 and 2 together with predictions from data for vibrational excitation by resonant electron collisions. It should be noted, that here and in the following particle densities are always normalized to one, i.e. they are divided by the gas density.

As (1) is motivated by the excitation processes in the discharge it is not adequate to describe the afterglow. Therefore, there only the population differences $\Delta N_v = N_v - N_{v+1}$ are inferred from the CARS spectra and the individual population densities are obtained by extrapolating the number density of the upper state of the highest detectable transition. For more details see [9]. Some results are shown in section 3.2 where they are compared with a simple volume averaged model for the vibrational system.

3. Description of the vibrational dynamics

3.1. Discharge phase

The two-temperature distribution function in equation (1) was already introduced in [9] but not further motivated. This shall be done here.

The main concept of equation (1) is that the nitrogen molecules can be divided into two mostly independent populations

$$N(v,J) = N_{\mathrm{c}}(v,J;T_{\mathrm{rot}},T_{\mathrm{vib,c}},R_{\mathrm{h}}) + N_{\mathrm{h}}(v,J;T_{\mathrm{rot}},T_{\mathrm{vib,h}},R_{\mathrm{h}}) \quad (5)$$

where the population of the vibrationally cold molecules is characterized by the cold temperature $T_{\mathrm{vib,c}}$ and the population of the hot molecules by the hot temperature $T_{\mathrm{vib,h}}$. Both populations share the same rotational temperature T_{rot} and the fraction of hot and cold molecules compared to the total amount of nitrogen is given by R_{h} and $(1-R_{\mathrm{h}})$, respectively.

On time scales of the nanosecond pulse there is essentially no exchange of vibrational excitation among the nitrogen molecules as V–V and V–T collisions are important only on longer time scales. The dominant process of vibrational excitation during the discharge is most certainly excitation by resonant electron collisions [1]. This leads to the following interpretation of the two distributions: N_{c} is the steady-state background distribution which comprises the bulk of the nitrogen molecules. During the discharge some molecules are transferred from N_{c} to N_{h} by electron collisions. This means the total excitation rate $\dot{R}_{\mathrm{h}}$ and the vibrational temperature of the newly excited molecules are solely defined by the corresponding cross sections, the electron density and the electron temperature.

For the analysis of the measurements in [9] the cross section and rate dataset calculated by Laporta *et al* [11–13]—freely accessible in the Phys4Entry database [14]—is used. First the characteristics of the hot distribution are investigated. While in (1) a Boltzmann distribution is assumed, there is no obvious physical reason which suggests this choice. To see, that the Boltzmann distribution is still a reasonably good approximation for the range of vibrational states visible in this work, in the following the excitation process is investigated. To begin we assume, that the electron conditions during most of the discharge are essentially constant. This is motivated by the constant electric field in [9] and the nearly constant current. So the rate equation for a vibrational state $v \geq 1$ is given by

$$\dot{N}_v = \sum_{i \neq v} N_i k(i,v;T_{\mathrm{e}}) n_{\mathrm{e}}, \quad (6)$$

where n_{e} is the electron density and $k(i,v;T_{\mathrm{e}})$ is the rate coefficient for the resonant excitation by electron collisions from

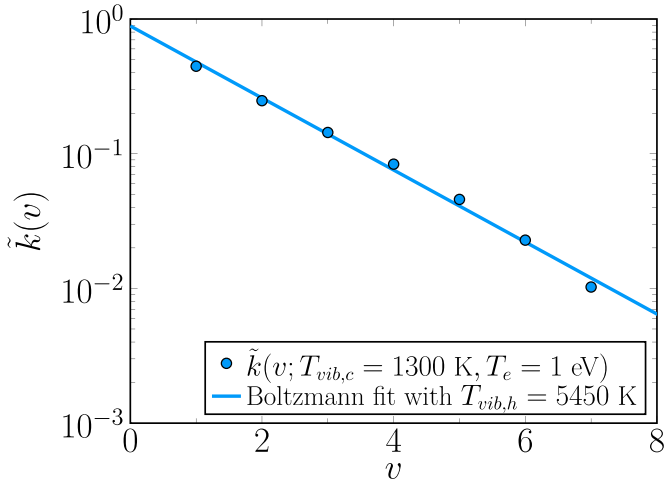

Figure 2. Sum of excitation rates into vibrational states v for an electron temperature of $T_\mathrm{e} = 1$ eV and a vibrational background with a (vib.) temperature of 1300 K (normalized by $\sum_v \tilde{k}(v)$). The solid line is a Boltzmann distribution with a temperature of 5450 K.

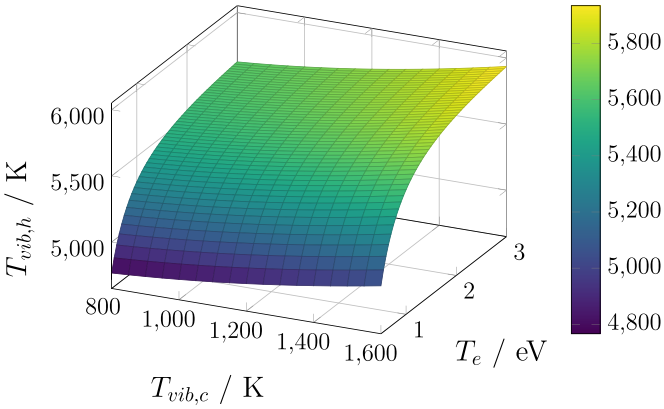

Figure 3. Temperature of the newly excited states in dependence of electron and vibrational temperature before the discharge.

vibrational state i to v at the electron temperature T_e. Here, the interest is only in the vibrational dynamics, so particle densities N_v can be understood as integrated over the rotational quantum number. Now, we distinguish between the newly excited molecules (i.e. the ones which are excited during the current discharge pulse) $\tilde{N}_v$ and the bulk of the molecules N_i which follows the cold distribution with temperature $T_\mathrm{vib,c}$. It is assumed that the number of bulk molecules is much larger than the number of molecules excited during the discharge, $\sum_v \tilde{N}_v \ll \sum_i N_i$, and therefore superelastic collisions can be ignored as their frequency scales with $\tilde{N}_v$. For constant n_e and T_e the solution of equation (6) for $\tilde{N}_v$ with the initial condition $\tilde{N}_v(t=0) = 0$ and under the assumption that the cold background stays constant, $N_v(t) = \mathrm{const}$, is trivial, and we find that

$$\begin{aligned} \tilde{N}_v &= \left(\textstyle\sum_{i<v} N_i k(i,v;T_\mathrm{e})\right) n_\mathrm{e} t \\ &\propto \textstyle\sum_{i<v} N_i(T_\mathrm{vib,c}) k(i,v;T_\mathrm{e}) =: \tilde{k}(v;T_\mathrm{vib,c},T_\mathrm{e}) \\ &\Rightarrow \tilde{N}_v \propto \tilde{k}(v;T_\mathrm{vib,c},T_\mathrm{e}). \end{aligned} \tag{7}$$

This means, that the shape of the distribution of the hot molecules is constant during the discharge and follows from the values of the corresponding rates. The sum of rates for all resonant electron processes into the vibrational states v are depicted in figure 2 for an exemplary electron temperature of $T_\mathrm{e} = 1$ eV and a background temperature of 1300 K, which is close to the values measured in [9]. As can be seen in figure 2, the rates, and therefore populations of the excited states, follow a similar dependency on the vibrational quantum number v as a Boltzmann distribution. This motivates the use of a Boltzmann distribution for the newly excited molecules. In this regard two points should be noted. First, the approximation with a Boltzmann distribution is not necessarily usable for conditions other than investigated in this work. For states $v > 7$ in nitrogen significant deviations from a Boltzmann distribution are and also no statements are made for other gases here. Second, there is no explicit physical motivation behind the use of the Boltzmann distribution. Instead, it was chosen because the concept of temperatures is convenient and familiar. By more detailed examination of the resonant processes leading to vibrational excitation a more precise distribution might be found, which is valid in regimes where this simple approximation fails. But for the purpose of this work a Boltzmann distribution is sufficient to describe the observed CARS spectra.

As presented in figure 2 the temperature of the hot molecules can be obtained by a fit to the rates from [11] for a given vibrational temperature of the molecule bulk and electron temperature. In figure 3 values for $T_\mathrm{vib,h}$ calculated in this way are shown for a range of $T_\mathrm{vib,c}$ and T_e. As can be seen the dependence on the vibrational bulk temperature is weak and decreases further for higher electron temperatures.

For a comparison of the theoretical $T_\mathrm{vib,h}$ the electron temperature is estimated with BOLSIG+ [15] and the IST Lisbon cross section data set [16] to be around 1.2 eV for the measured reduced electric field of 81 Td. As the dependency on $T_\mathrm{vib,c}$ is weak (see figure 3), in figure 5 the measurements are only compared to the theoretical value for $T_\mathrm{vib,c} = 1300$ K. Considering the drastic simplifications in the derivation of the theoretical value and the measurement uncertainty generally a good agreement can be observed.

In addition to the temperature of the newly excited molecules it is possible to estimate the rate of excitation. The parameter R_h in (1) describes the total amount of newly excited molecules relative to the gas density. With (6) one obtains

$$\dot{R}_\mathrm{h} = \frac{\partial}{\partial t}\left(\sum_{v>0} \tilde{N}_v\right) = \sum_{v>0} \tilde{k}(v;T_\mathrm{vib,c},T_\mathrm{e}) n_\mathrm{e} \tag{8}$$

for the derivative of R_h. In figure 4 the dependence of $\dot{R}_\mathrm{h}/n_\mathrm{e}$ is shown in a similar fashion as it is done for the temperature in figure 3, and it can be seen that there is essentially no dependence on the initial temperature for the excitation rate. Strictly speaking, (8) is only valid in the beginning of the discharge

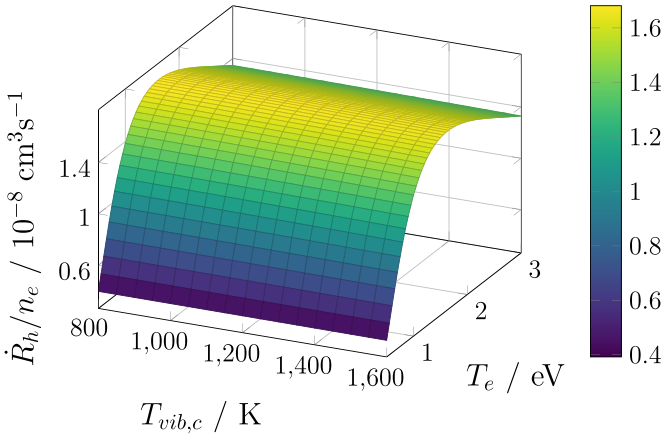

Figure 4. Dependence of $\dot{R}_h/n_e$ on the temperature of the cold molecules and the electrons.

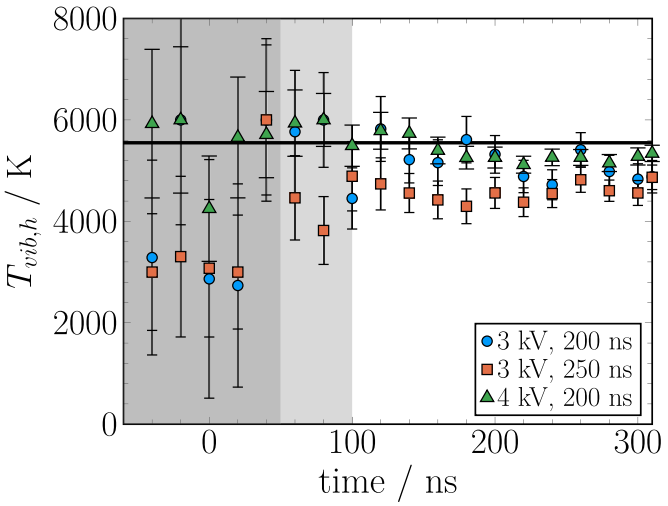

Figure 5. Temperature of the newly excited molecules obtained by the CARS measurements [9]. For the measurement with 4 kV and with 3 kV applied voltage, the dark gray and the light gray shaded regions should not taken into account, respectively [9]. The solid line corresponds to the theoretical value for a vibrational bulk temperature of 1300 K and a electron temperature of 1.2 eV (corresponding to a reduced electric field of 81 Td according to BOLSIG+ calculations [15] with the IST Lisbon data set [16]).

as it depends on the approximation $R_h \ll 1$. In our measurements we see an increase of R_h up to about 0.1. Therefore, some minor correction need to be applied to (8). To account for the depletion of the cold background N_i in (7) is multiplied by $(1-R_h)$. Additionally, when R_h increases the possibility of multiple vibrational excitation processes can become important. If molecules from R_h are excited again and end up in states higher than the highest state visible in the CARS spectra, v_{max}, they cannot be seen in the measurement. Therefore, an effective loss rate $k_{loss}(v;R_h,T_{vib,h},T_e)$ is introduced. With these corrections (8) becomes

$$\dot{R}_h = \sum_{v>0}\Big[\tilde{k}'(v,R_h;T_{vib,c},T_e)n_e - k_{loss}(v,R_h;T_{vib,h},T_e)n_e\Big], \quad (9)$$

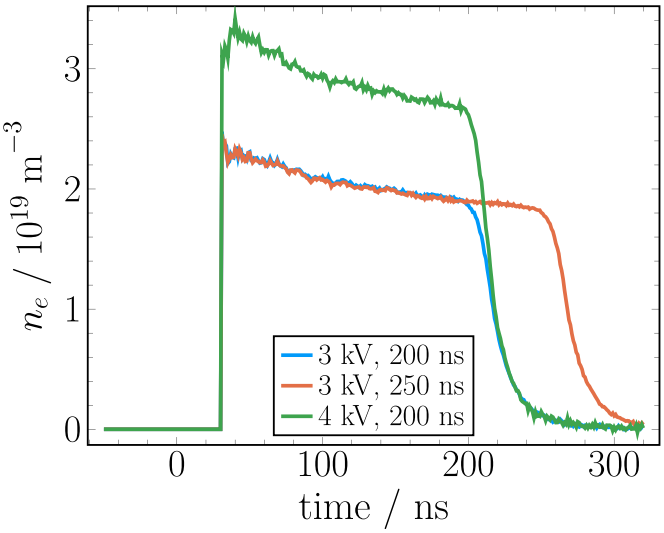

Figure 6. Electron density obtained from (12). The first 20 ns are not included, as at that time the electric field is unknown. This should be uncritical for the analysis of the vibrational dynamics, because the electric field during this time should be too high for efficient vibrational excitation.

where $\tilde{k}'$ and k_{loss} can both be expressed analog to the definition of the TTDF (1) as

$$\tilde{k}'(v,R_h;T_{vib,c},T_e) = \sum_{i<v} k(i,v;T_e)\frac{1-R_h}{Z'_c}e^{-\frac{E(i,0)-E(0,0)}{k_B T_{vib,c}}} \quad (10)$$

and

$$k_{loss}(v,R_h;T_{vib,h},T_e) = \sum_{j>v_{max}} k(v,j;T_e)\underbrace{\frac{R_h}{Z'_h}e^{-\frac{E(v,0)-E(0,0)}{k_B T_{vib,h}}}}_{\text{for } v>0}. \quad (11)$$

Here, the corresponding distributions are summed over the rotational quantum number which is reflected in the partition functions Z'_c and Z'_h. Note, that because $T_{vib,h}(T_{vib,c},T_e)$, (10) is not more complex than (8) in the sense, that it still depends only on the external parameters n_e, $T_{vib,c}$ and T_e.

As the electric field is constant during the current plateau the electron density can be calculated from the measured current from

$$\frac{I(t)}{A} = \mu(E)En_e(t) \quad (12)$$

where $I(t)$ is the current measured in the plateau, E is the electric field obtained by the E-FISH measurements [9] and A is the plasma cross section. During the high current pulse in the beginning the electric field can be much higher than in the plateau [17]. Therefore, (12) is only evaluated for $t > 20$ ns, i.e. during the plateau phase. The resulting electron densities are shown in figure 6.

In figure 7 the theoretical R_h—calculated by integrating (10)—is compared to the measured values of R_h during the discharge pulse. The initial value for the integration is chosen to be the average of the three data points before the ignition of the discharge ($t \leq 0$ ns). A very good agreement

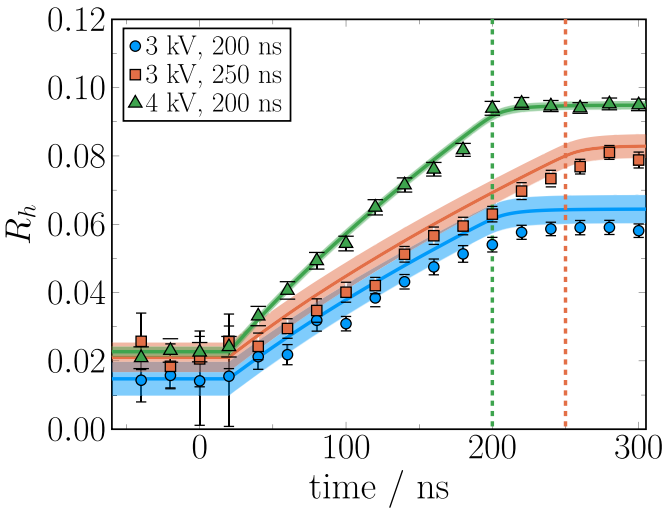

Figure 7. Fraction of the newly excited molecules during the discharge pulse [9]. The solid lines are the theoretical rates calculated with the data from [11] for electron temperatures and densities obtained by current and field measurements for 4 kV applied voltage (green) and 3 kV (blue). The shaded ribbons give the uncertainty due to the uncertainty in the initial values.

is observed between the measurements and the theoretical values calculated from the current and field measurements even though those are completely independent of the CARS measurements.

3.2. Afterglow

To analyze the dynamics of vibrationally excited states in the afterglow between two discharge pulses a kinetic model is developed for vibrationally excited nitrogen up to $v = 9$.

As the ionization degree is very low, superelastic collisions with the plasma electrons are neglected here. Furthermore, the influence of electronically excited molecules is ignored and the dissociation degree is assumed to be small. These assumptions reduce the reaction set to V–V and V–T collisions among the nitrogen molecules.

The rates for the V–V process

$$\mathrm{N_2}(v+1) + \mathrm{N_2}(w) \rightarrow \mathrm{N_2}(v) + \mathrm{N_2}(w+1) \tag{13}$$

are calculated from the rate for the process

$$\mathrm{N_2}(1) + \mathrm{N_2}(0) \rightarrow \mathrm{N_2}(0) + \mathrm{N_2}(1) \tag{14}$$

via the scaling law of the semiclassical forced harmonic oscillator model [18, 19]

$$\begin{aligned} &k_{VV}(v+1, w \rightarrow v, w+1) \\ &= k_{VV}(1,0 \rightarrow 0,1)(v+1)(w+1)\frac{3-\mathrm{e}^{-\frac{2\lambda}{3}}}{2}\mathrm{e}^{-\frac{2\lambda}{3}}\exp\left(\frac{\Delta E}{2k_\mathrm{B}T}\right) \end{aligned} \tag{15}$$

where k_B is the Boltzmann constant and T the gas temperature. λ is given by [19]

$$\lambda = \frac{1}{3\sqrt{2}}\sqrt{\frac{\theta}{T}}\frac{|\Delta E|}{\omega\hbar} \tag{16}$$

with the harmonic angular frequency ω and $\theta = \frac{4\pi^2\omega^2 m}{\alpha^2 k_\mathrm{B}}$. $\Delta E = E(v+1) + E(w) - E(v) - E(w+1)$ is the energy defect due to the anharmonicity of the vibrational potential, m is the collisional reduced mass and α is the exponential repulsive potential parameter [19]. For $k_{VV}(1,0 \rightarrow 0,1)$ the value 0.9×10^{-14} $\mathrm{cm^3\ s^{-1}}$ is used [20].

For completeness the V–T rates from the calculations provided by Billing and Fisher [20] for a (rotational-translational) gas temperature of 300 K are included. It should be noted that they are several orders of magnitude smaller and do not affect the simulation in a noticeable way.

The simulation volume is one half of the discharge jet, i.e. a cuboid with edge lengths 1 mm× 1 mm× 10 mm. As first approximation the particle densities are assumed to be homogeneous in the entire volume. The influx of is considered via [21]

$$\left.\frac{\partial N_0}{\partial t}\right|_\mathrm{in} = N_\mathrm{gas}\frac{CQP_\mathrm{atm}}{VP} \tag{17}$$

where $Q = 10$ sccm is half of the set gas flow—as it is assumed that the total gas flow of 20 sccm is split equally to both sides of the jet. $C = 1.6667 \times 10^{-8}$ $\mathrm{m^3\ s^{-1}\ sccm^{-1}}$ is the conversion factor to convert sccm to $\mathrm{m^3\ s^{-1}}$, $P_\mathrm{atm} = 1$ bar is the atmospheric pressure, $P = 200$ mbar is the pressure in the discharge chamber and N_gas is the gas density. In (17) it is assumed, that the inflowing particles are all in the vibrational ground state as at room temperature there is no significant vibrational excitation. The vibrational excited nitrogen molecules in state v exiting the jet are described by

$$\left.\frac{\partial N_v}{\partial t}\right|_\mathrm{out} = -N_v\frac{CQP_\mathrm{atm}}{VP}. \tag{18}$$

The loss of excited molecules by diffusion to the walls is given by [21, 22]

$$\begin{aligned} \left.\frac{\partial N_{v>0}}{\partial t}\right|_W &= -N_{v>0}\left(\frac{\Lambda_0^2}{D_v} + \frac{2(2-\gamma_v)V}{v_\mathrm{th}\gamma_v A}\right)^{-1} \\ &\approx -N_{v>0}\frac{v_{th}\gamma_v A}{2(2-\gamma_v)V} \end{aligned} \tag{19}$$

with the characteristic length scale for the given geometry Λ_0 [22], the volume and surface area V and A, the diffusion coefficient for the species D_v and the corresponding deactivation coefficient γ_v giving the probability to lose a particle in state v when it hits the wall. γ_v is not very well known for states $v > 1$ but for $v = 1$ it is typically in the order of about 4×10^{-4} to 3×10^{-3} for different materials [23]. In absence of better knowledge the deactivation coefficient is chosen here to be $\gamma = 1 \times 10^{-3}$ for all states. This motivates the approximation in (19) which is consistent with the assumption of flat density profiles: the very low deactivation coefficient means that

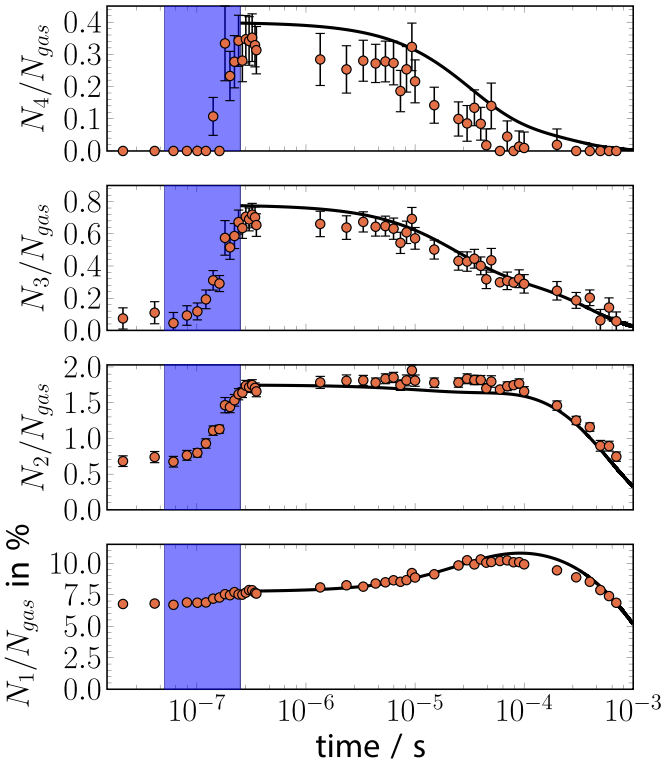

Figure 8. Relative population densities for the measurement 3 kV, 200 ns. Symbols are the population densities obtained with the method described in [9] and lines are the results from the kinetic model.

the loss of excited particles is not limited by the diffusion, but instead by the deactivation process once the molecules reach the walls. Finally, we assume that the deactivation happens directly into the ground state, so that the walls are effectively a source for $v = 0$:

$$\left.\frac{\partial N_0}{\partial t}\right|_W = -\sum_{v>0} \left.\frac{\partial N_v}{\partial t}\right|_W . \tag{20}$$

With (18) and (19) one can compare the relative importance of the two transport loss terms, with the result that even with the low deactivation coefficient losses due to deactivation at the walls are six times higher, than the losses due to the gas flow out of the discharge.

The initial conditions for the simulation are obtained from the two-temperature distribution directly after the discharge pulse. In this way the initial population densities are extrapolated up to $v = 9$. The results of the simulation are compared to the measurement results from [9] in figure 8. For clarity of presentation the results for the other two measurement conditions are shown in the appendix (see figures A1 and A2). Those show a similar good agreement.

From the very good agreement between the measurements and the simple simulation it can be inferred, that here the E–V transitions, i.e. population of vibrational states by deexcitation of electronically excited molecules, seem to play only a minor role in contrast to previous works [7, 8]. A possible reason to explain this difference could be a generally higher electric field in discharges therein, which increases the amount of electronic excitation. While there is not much information about the discharge used by Deviatov *et al* [7], Montello *et al* [8] used a pin-to-pin discharge with a 10 mm gap. Their estimated electric field reaches up to about 275 Td during the ignition phase and stays at about 125 Td during the discharge plateau which is significantly higher than the value obtained by E-FISH measurements [9] in the discharge investigated here. Additionally, their pulse is only 150 ns long, which further increases the relative importance of the high electric field during the ignition. Therefore, it is very likely, that in their discharges the density of electronically excited states relative to the vibrationally excited states is significantly higher.

4. Conclusions

In this paper, the vibrational two-temperature distribution function used in the companion Paper [9] to evaluate CARS spectra during a ns-pulsed discharge was motivated and the different parameters were connected to the underlying physical processes. It is found that under the investigated discharge conditions the direct resonant excitation through electron collisions is the main path for production of vibrationally excited nitrogen. The distribution function of the newly excited molecules follows therefore the shape of the corresponding excitation probabilities or rates. In the case of the resonant excitation, investigated in this work, this shape closely resembles a Boltzmann distribution for small v, leading to the two-temperature distribution function (1) consisting of a Boltzmann distributed cold background and the also Boltzmann distributed newly excited hot molecules. For the case that the excitation rates do not follow a Boltzmann distribution, the hot part of the distribution function can be modified easily. If sufficient data for the excitation process is known the parameter in the distribution function can be estimated, and it is found that the estimates—using the rates reported by Laporta [11] in combination with current and field measurements—agree very well with the measured values. This shows that the rather simple two-temperature distribution—and its generalization by allowing non-Boltzmann distributions—provides a useful framework for analyzing and potentially optimizing the vibrational excitation of molecules in plasmas where the resonant excitation by electron collisions is the dominant process. Furthermore, the fact that the current and electric field are nearly constant during almost the entire high voltage pulse for the discharge type investigated in this work, indicates a constant electron density during the majority of the discharge which is created essentially only during the ignition of the pulse. The same behaviour is also seen for different molecular species, e.g. hydrogen [24–26]. This promises an easy tool for estimating the amount of vibrational excitation *a priori*, when one is able to predict the density and electric field for the given discharge.

For the afterglow it was found, that a relative simple model considering only V–V and V–T transfer and transport losses is enough to reproduce the measurements. Meaning E–V transfer—where vibrational excited molecules in the

electronic ground state are produced by cascades or quenching of higher electronic states—seems to be of minor importance in this discharge type. A possible reason why E–V transfer was needed to explain previous vibrational measurements [7, 8] could be the generally higher electric field in those works.

Finally, it can be concluded that the discharge reactor investigated here shows promise to be a handy tool while investigating the influence of vibrational excitation for example on plasma chemistry or plasma catalysis. Together with the description of the vibrational system provided here it allows to easily control and understand the vibrational excitation in the plasma volume, which is vital to understand its influence on other reactions.

Data availability statement

The data that support the findings of this study are available upon reasonable request from the authors.

Acknowledgment

This project is supported by the DFG (German Science Foundation) within the framework of the CRC (Collaborative Research Centre) 1316 ‘Transient atmospheric plasmas—from plasmas to liquids to solids’.

Appendix A. Additional simulation results

For completeness here the results of the simulation are compared to the measurements ‘3 kV, 200 ns’ and ‘4 kV, 200 ns’ from [9] in figures A1 and A2. The agreement is as good as in figure 8, leading to the conclusion, that for all conditions investigated the processes included in the simulation are sufficient to explain the experimental results.

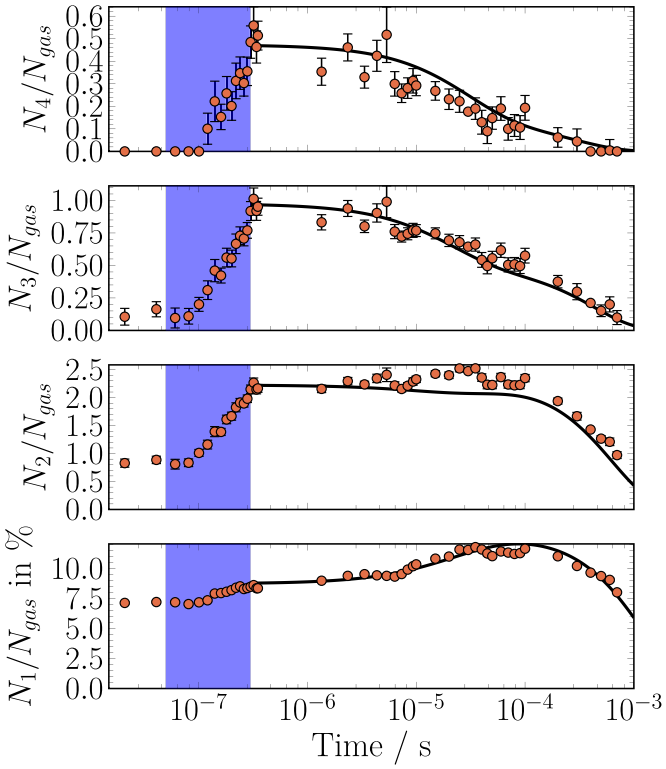

Figure A1. Relative population densities for the measurement 3 kV, 250 ns. Symbols are the population densities obtained with the method described in [9] and lines are the results from the kinetic model.

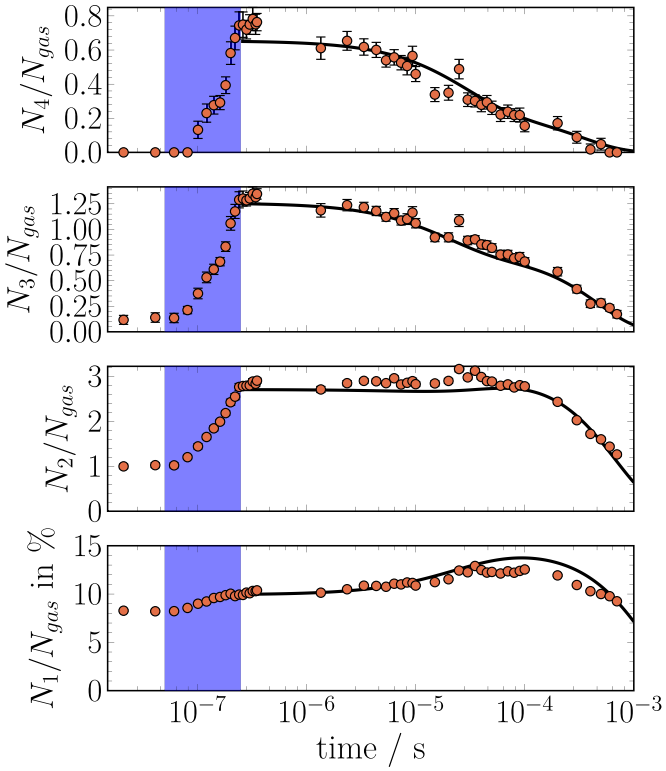

Figure A2. Relative population densities for the measurement 4 kV, 200 ns. Symbols are the population densities obtained with the method described in [9] and lines are the results from the kinetic model.

ORCID iDs

J Kuhfeld https://orcid.org/0000-0003-2335-2634
U Czarnetzki https://orcid.org/0000-0002-5823-1501

References

[1] Fridman A A 2008 *Plasma Chemistry* first paperback edn (Cambridge: Cambridge University Press)
[2] Neyts E C and Bogaerts A 2014 Understanding plasma catalysis through modelling and simulation—a review *J. Phys. D: Appl. Phys.* **47** 224010
[3] Whitehead J C 2016 Plasma–catalysis: the known knowns, the known unknowns and the unknown unknowns *J. Phys. D: Appl. Phys.* **49** 243001
[4] Lempert W R and Adamovich I V 2014 Coherent anti-Stokes Raman scattering and spontaneous Raman scattering diagnostics of nonequilibrium plasmas and flows *J. Phys. D: Appl. Phys.* **47** 433001
[5] Eckbreth A C 1996 *Laser Diagnostics for Combustion Temperature and Species* (*Laser Diagnostics for Combustion Temperature and Species*) vol 3 2nd edn (Boca Raton, FL: CRC Press)
[6] Shaub W M, Nibler J W and Harvey A B 1977 Direct determination of non-Boltzmann vibrational level populations in electric discharges by CARS *J. Chem. Phys.* **67** 1883–6
[7] Deviatov A A, Dolenko S A, Rakhimov A T, Rakhimova T V and Roi N N 1986 Investigation of kinetic processes in molecular nitrogen by the CARS technique *Zh. Eksp. Teor. Fiz.* **90** 429–36
[8] Montello A, Yin Z, Burnette D, Adamovich I V and Lempert W R 2013 Picosecond CARS measurements of nitrogen vibrational loading and rotational/translational temperature in non-equilibrium discharges *J. Phys. D: Appl. Phys.* **46** 464002
[9] Kuhfeld J, Lepikhin N D, Luggenhölscher D and Czarnetzki U 2021 Vibrational CARS measurements in a near-atmospheric pressure plasma jet in nitrogen: I. Measurement procedure and results *J. Phys. D: Appl. Phys.* **54** 305204
[10] Messina D, Attal-Trétout B and Grisch F 2007 Study of a non-equilibrium pulsed nanosecond discharge at atmospheric pressure using coherent anti-Stokes Raman scattering *Proc. Combustion Institute* vol 31 pp 825–32
[11] Laporta V, Little D A, Celiberto R and Tennyson J 2014 Electron-impact resonant vibrational excitation and dissociation processes involving vibrationally excited N_2 molecules *Plasma Sources Sci. Technol.* **23** 065002
[12] Laporta V, Celiberto R and Wadehra J M 2012 Theoretical vibrational-excitation cross sections and rate coefficients for electron-impact resonant collisions involving rovibrationally excited N_2 and NO molecules *Plasma Sources Sci. Technol.* **21** 055018
[13] Laporta V and Bruno D 2013 Electron-vibration energy exchange models in nitrogen-containing plasma flows *J. Chem. Phys.* **138** 104319
[14] PHYS4ENTRY (7th Framework Programme) (available at: https://users.ba.cnr.it/imip/cscpal38/phys4entry/database.html)
[15] Hagelaar G J M and Pitchford L C 2005 Solving the Boltzmann equation to obtain electron transport coefficients and rate coefficients for fluid models *Plasma Sources Sci. Technol.* **14** 722–33
[16] Alves L L 2014 The IST-LISBON database on LXCat *J. Phys.: Conf. Ser.* **565** 012007
[17] Lepikhin N D, Luggenhölscher D and Czarnetzki U 2020 Electric field measurements in a He:N_2 nanosecond pulsed discharge with sub-ns time resolution *J. Phys. D: Appl. Phys.* **54** 055201
[18] Adamovich I V 2001 Three-dimensional analytic model of vibrational energy transfer in molecule-molecule collisions *AIAA J.* **39** 1916–25
[19] Ahn T, Adamovich I V and Lempert W R 2004 Determination of nitrogen V–V transfer rates by stimulated Raman pumping *Chem. Phys.* **298** 233–40
[20] Billing G D and Fisher E R 1979 VV and VT rate coefficients in N_2 by a quantum-classical model *Chem. Phys.* **43** 395–401
[21] Kemaneci E, Carbone E, Booth J P, Graef W, van Dijk J and Kroesen G 2014 Global (volume-averaged) model of inductively coupled chlorine plasma: influence of Cl wall recombination and external heating on continuous and pulse-modulated plasmas *Plasma Sources Sci. Technol.* **23** 045002
[22] Chantry P J 1987 A simple formula for diffusion calculations involving wall reflection and low density *J. Appl. Phys.* **62** 1141–8
[23] Black G, Wise H, Schechter S and Sharpless R L 1974 Measurements of vibrationally excited molecules by Raman scattering. II. Surface deactivation of vibrationally excited N_2 *J. Chem. Phys.* **60** 3526–36
[24] Donkó Z, Schulze J, Müller S and Czarnetzki U 2011 Kinetic simulation of a nanosecond-pulsed hydrogen microdischarge *Appl. Phys. Lett.* **98** 251502
[25] Lo C and Hamaguchi S 2011 Dynamics of near-atmospheric-pressure hydrogen plasmas driven by pulsed high voltages *IEEE Trans. Plasma Sci.* **39** 2100–1
[26] Lo C W and Hamaguchi S 2011 Numerical analyses of hydrogen plasma generation by nanosecond pulsed high voltages at near-atmospheric pressure *J. Phys. D: Appl. Phys.* **44** 375201